Supplementary Material (ESI) for Physical Chemistry Chemical Physics

Supplementary Information

Unfolding Dynamics of Cytochrome *c* Revealed by Single-Molecule and Ensemble-Averaged Spectroscopy

Jungkweon Choi, Sooyeon Kim, Takashi Tachikawa, Mamoru Fujitsuka, and Tetsuro Majima*

MALDI-TOF mass spectrum of Apocytochrome c

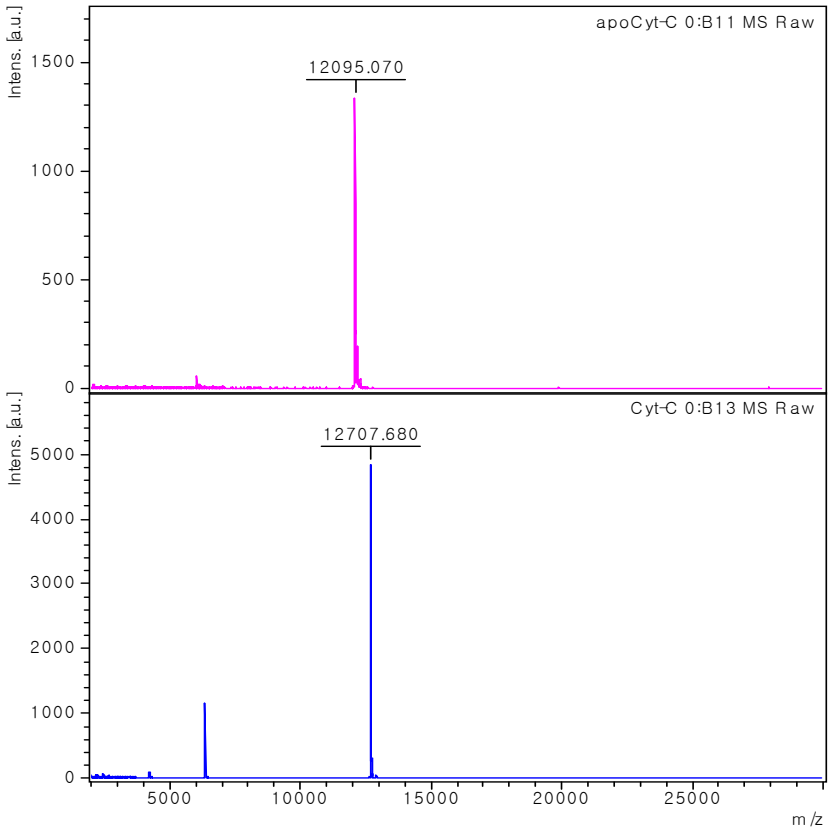

Fig. S1. Mass spectra of ApoCyt*c* (upper) and WT Cyt*c* (lower).

Fluorescence lifetimes of Cytc-A488 and Alexa 488 with various concentrations of GdHCl (Bulk experiments)

All the decay profiles measured from Alexa 488 can be fitted by a single exponential function with relaxation times of 3.8 ± 0.1 ns (see Fig. S3b). In contrast, all fluorescence decay profiles measured from Cyt*c*-A488 at various GdHCl concentrations can be expressed by a bi-exponential function. By a simple analysis of all the fluorescence decay profiles, we found three components with different fluorescence lifetimes in the GdHCl-induced unfolding reaction of Cyt*c*-A488. Thus, we fitted all the decay profiles of Cyt*c*-A488 with a tri-exponential function. A global fitting analysis revealed three relaxation times of 0.36, 0.81, and 3.21 ns in the GdHCl-induced unfolding reaction of Cyt*c*-A488.

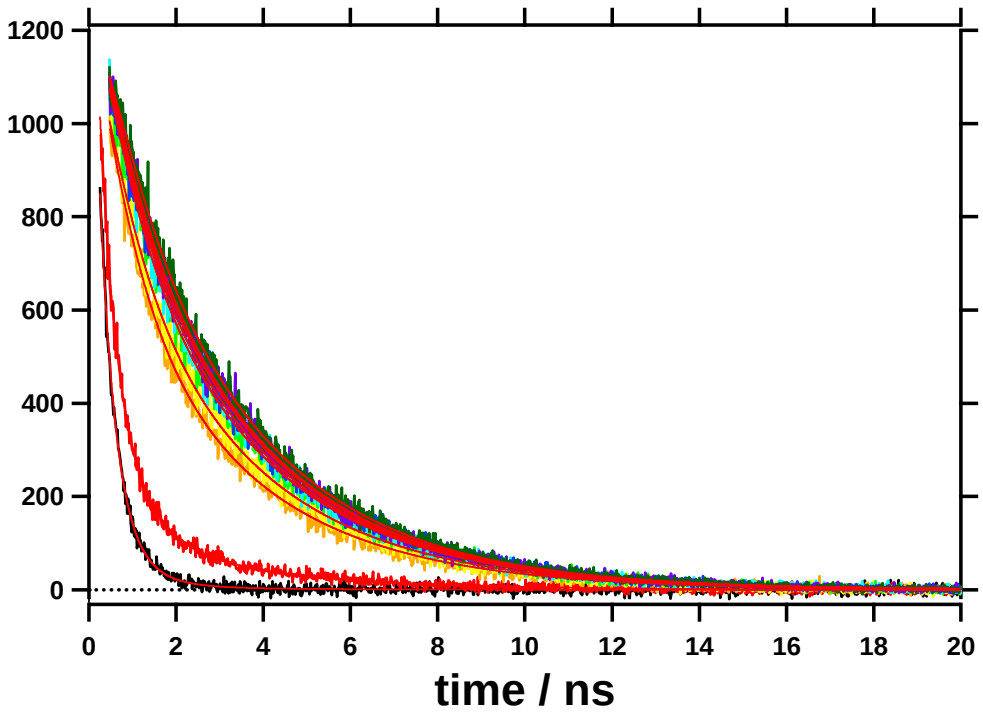

Fig. S2. Global fitting results of the fluorescence decay profiles of Cyt*c*-A488 as a function of the concentration of GdHCl. All decay profiles of Cyt*c*-A488 were expressed by a tri-exponential function with relaxation times of 0.36, 0.81, and 3.21 ns. The theoretical fits obtained from the fitting analysis are shown in red.

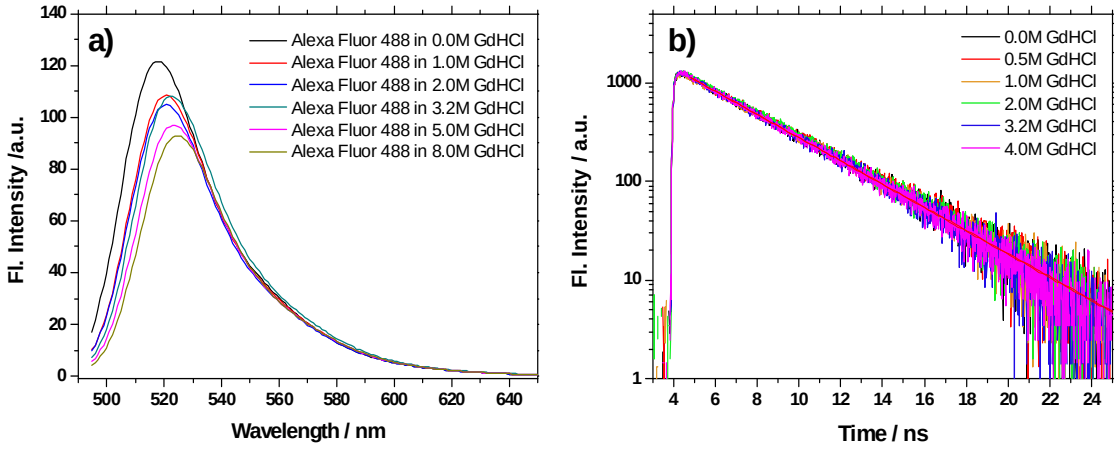

Fig. S3. a) Fluorescence spectra of Alexa 488 as a function of the concentration of GdHCl in 100 mM phosphate buffer. b) The fluorescence decay profiles of Alexa 488 as a function of the concentration of GdHCl in 100 mM phosphate buffer (pH 7.0).

Transient absorption measurement

The sub-picosecond transient absorption spectra were measured by the pump and probe method using a regeneratively amplified titanium sapphire laser (Spectra Physics, Spitfire Pro F, 1 kHz) pumped by a Nd:YLF laser (Spectra Physics, Empower 15) for an aqueous solution containing Cyt*c*-A488 or Alexa 488 in 100 mM Na phosphate buffer (pH 7.0). The seed pulse was generated by the titanium sapphire laser (Spectra Physics, Tsunami 3941-M1BB, full width at half-maximum 80 fs,

800 nm). An excitation pulse at 485 nm was generated by optical parametric amplifier (Spectra Physics, OPA-800CF). A white continuum pulse, which was generated by focusing the residual of the fundamental light to a flowing water cell after a computer controlled optical delay, was divided into two parts and used as the probe and the reference lights, of which the latter was used to compensate the laser fluctuation. Both probe and reference lights were directed to a rotating sample cell with 1.0 mm of optical path and were detected with a charge-coupled device detector equipped with a polychromator (Solar, MS3504). The pump pulse was chopped by a mechanical chopper synchronized to one-half of the laser repetition rate, resulting in a pair of the spectra with and without the pump, from which an absorption change induced by the pump pulse was estimated.

By the femtosecond transient absorption measurement, we found that the transient absorption spectra of Cyt*c*-A488 obtained after 485 nm laser excitation without GdHCl are similar to that of Alexa 488. These spectra display the transient absorption signal at around 430 nm and the broad bleaching signal due to the absorption band and emission of Alexa 488, respectively. The transient signal of Cytc-A488 observed at 430 nm certainly originates from the formation and decay of the excited singlet state of Alexa 488. However, we could not observe any dynamics due to energy transfer between Alexa 488 and heme, as shown in Fig. 4a and S4.

On the other hand, we have to consider photoinduced electron transfer (PET) between Alexa 488 to the iron ion of the heme in Cyt*c*-A488. As shown in Fig. S6, the absorption band of the reduced Cyt*c* is very different with that of the oxidized Cyt*c*. Thus, if PET from Alexa 488 to the iron ion of the heme occurs in this system, the transient absorption band of the reduced Cyt*c* generated by PET should be observed. However, we could not observe any signal related to PET between Alexa 488 and heme. This result means that PET from Alexa 488 to the iron ion of the heme does not take place in this system. Thus, we conclude that the fluorescence quenching observed from the folded Cyt*c*-A488 is mainly due to PET between electron-donating amino acids such as tryptophan (Trp) and a dye attached to a protein rather than the energy transfer.

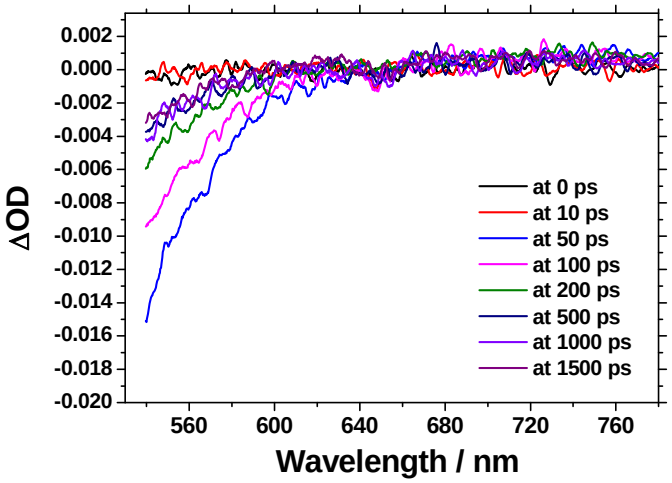

Fig. S4. Transient absorption spectra of Cyt*c*-A488 without GdHCl obtained after 485 nm laser excitation in 100 mM phosphate buffer.

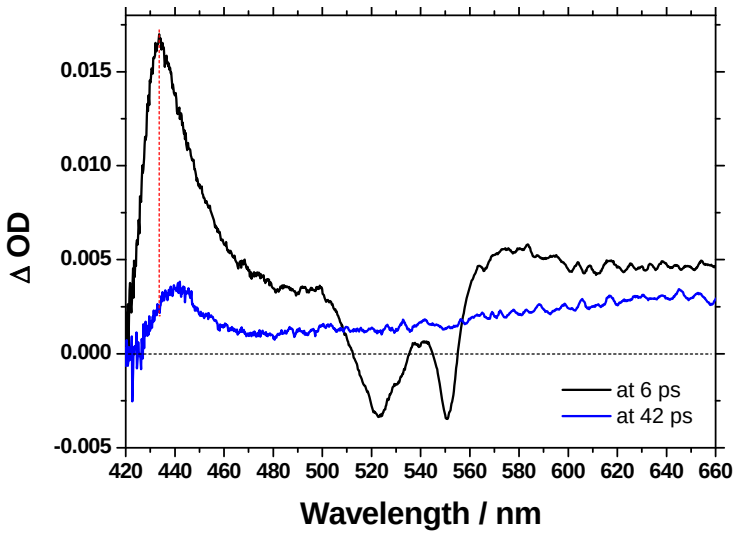

Fig. S5. Transient absorption spectra of WT Cyt*c* without GdHCl after 360 nm laser excitation in 100 mM phosphate buffer.

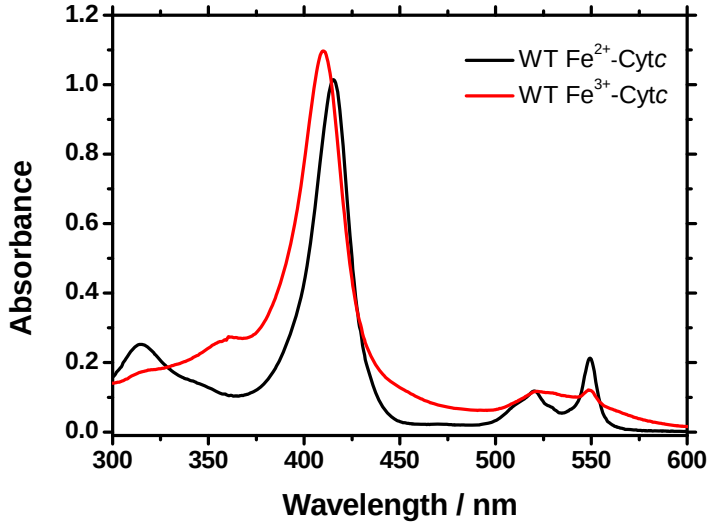

Fig. S6. Absorption spectra of the oxidized and reduced wide-type Cyt*c* without GdHCl in 100 mM phosphate buffer.

Fluorescence quenching of Alexa 488 by the addition of Trp

Fig. S7 shows that the fluorescence spectra of Alexa 488 as a function of the concentration of Trytophan (Trp) in 100 mM phosphate buffer. The fluorescence intensities of Alexa 488 were significantly decreased by increasing the concentration of Trp. The quenching constant k_q is determined from the Stern-Volmer plot as follows:

$$\frac{F_0}{F} = 1 + K_{SV}[\mathrm{Q}]$$

$$K_{SV} = k_q \tau_0$$

where F_0 and F are the fluorescence intensities in the absence and presence of quencher, respectively. [Q] is the concentration of the quencher (Trp). τ_0 is the lifetime of the fluorophore in the absence of quencher.

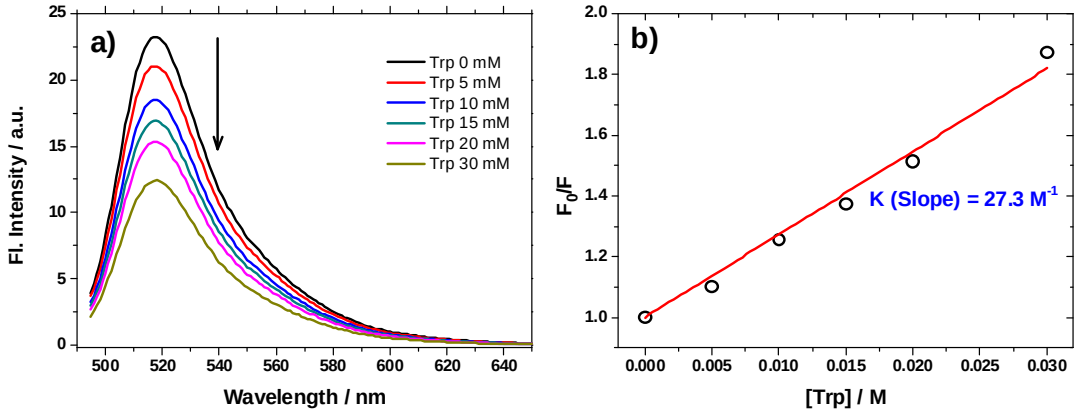

Fig. S7. a) Fluorescence spectra of Alexa 488 as a function of the concentration of Trytophan (Trp) in 100 mM phosphate buffer. b) Stern-Volmer plot of Alexa 488 quenched by Trp. ([Alexa 488] = 0.42 μM).

Fluorescence quenching mechanism

The fluorescence lifetime of Cyt*c*-A488 is significantly shorter in the absence of GdHCl than in its presence whereas the fluorescence lifetime of Alexa 488 is not affected by the addition of GdHCl. From the fs-transient absorption measurement and the fluorescence quenching of Alexa 488 by the addition of Trp, we found that PET take place dominantly between the attached Alexa 488 and amino acids such as Trp, and PET in the folded state of a protein is very efficient compared to that in the denatured state (See the section of the *transient absorption measurement and fluorescence quenching of Alexa 488 by the addition of Trp*). Indeed, Chen et al. reported that the fluorescence of Alexa 488 is quenched by the interaction with Trp, Tyr, Met and His residues through a combination of static and dynamic quenching mechanism.[2] They also show that electron transfer from Trp to Alexa 488 is highly favorable compared with other three residues. These results agree well with our results. Thus, we suggest that the fluorescence quenching of Cyt*c*-A488 by GdHCl is mainly due to PET from the electron donor (Trp) to Alexa 488.

Here, it is worthy to note that the fluorescence lifetime (3.27 ns) of the unfolded Cyt*c*-A488 is slightly shorter than that observed from free Alexa 488 (3.69 ns), indicating that there is another source for the fluorescence quenching of Alexa 488 in addition to PET between Alexa 488 and Trp. As suggested by Chen et al., the fluorescence quenching of Cyt*c*-A488 in the high concentration of GdHCl may be due to the interaction with Tyr, Met and His residues. Especially, Tyr 97 and Cys102 are located to the same helix and the distance between two residues is short as depicted in Fig. S8 (The distance between Tyr97 and cys102 is calculated to be 7.3Å from the crystal structure). Thus we suggest that the interaction between Alexa 488 and Tyr97 should induce fluorescence quenching even in the unfolded state as well as in the native state.

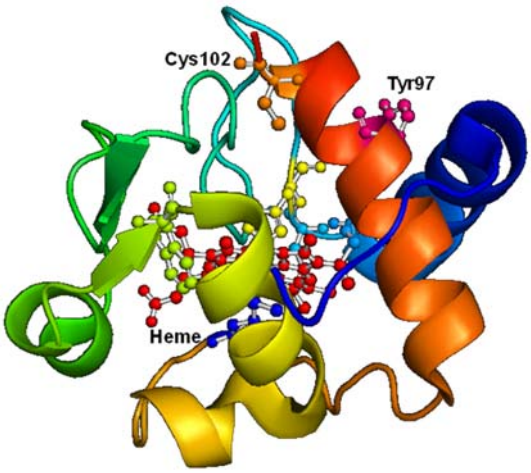

Fig. S8. Structure of Alexa 488-labeled yeast iso-1-cytochrome *c* (Cyt*c*-A488) (Yeast iso-1-Cytochrome *c*: PDB ID code 1YCC) showing the heme and the locations of residues. Alexa 488 is labeled to residue 102 (Cys102) of Cyt*c*. The distance between Cys102 (Orange) and Tyr97 (Pink) is calculated to be 7.3 Å from the crystal structure.

Fluorescence quenching of ApoCytc-A488 by the addition of GdHCl

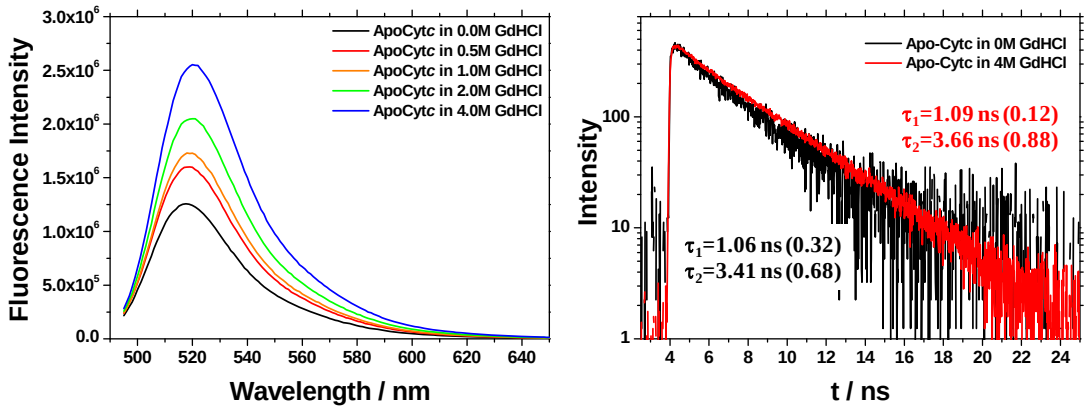

Fig. S9. a) Fluorescence spectra of ApoCyt*c*-A488 as a function of the concentration of GdHCl in 100 mM phosphate buffer. b) Fluorescence decay profiles of ApoCyt*c*-A488. The fluorescence lifetimes ($\langle\tau\rangle$) of Alexa 488 attached to ApoCyt*c* at 0 M and 4 M GdHCl were determined to be 2.66 ns and 3.35 ns, respectively.

Three-state model

In the three-state model, the native Cyt*c* (N) is unfolded through an intermediate (I).

$$N \xrightarrow{c_{m1},m_1} I \xrightarrow{c_{m2},m_2} U$$

At each concentration of the denaturant, the free energies for N→I and I→U transitions, ΔG_1 and ΔG_2, were calculated using the following equation:

$$\Delta G_1 = -RTln\left[\frac{x_N - x_i}{x_i - x_I}\right]$$

$$\Delta G_2 = -RTln\left[\frac{x_I - x_i}{x_i - x_U}\right]$$

where x_i is the numerical value of the structure-sensitive parameter at the *i*th denaturant concentration (i.e., the fluorescence intensity in this case); x_N, x_I and x_U are the numerical values of the same

parameter relative to the native, intermediate and completely unfolded states, respectively. The free energy changes for N→I and I→U transitions in the absence of denaturant ($\Delta G^0_{N\text{-}I}$ and $\Delta G^0_{I\text{-}U}$) and the $-m_1$ *and* $-m_2$ values were calculated from the plot of ΔG_{Obsd} as a function of [GdHCl] with an equation

$$\Delta G_{Obsd} = \Delta G^0_{N\text{-}I} + m[\text{GdHCl}]$$
$$\Delta G_{Obsd} = \Delta G^0_{I\text{-}U} + m[\text{GdHCl}]$$

Changes in $-m$ values are indicators of the change in solvent-exposed surface area upon each transition.

Single-molecule experiments with confocal laser scanning microscopy

In order to take the single-molecule image, solutions of Cyt*c*-A488 at 1 nM contained 1wt.% trehalose. Trehalose (α-D-glucopyranosyl-α-D-glucopyranoside) is well known as a stabilizer in single-molecule experiments. However, it also has a stabilizing effect on proteins that is opposite to the denaturing effect of GdHCl. Therefore, in this study trehalose was added to the sample solution at less than 1% (~25 mM)as a minimum quantity to minimize its stabilizing effect on proteins that is opposite to the denaturing effect of GdHCl. As a control experiment, we measured the fluorescence lifetimes of Cyt*c*-A488 and Alexa 488 with 1% trehelose in the bulk phase. As shown in Fig. S10a, the photophysical properties of Cyt*c*-A488 and Alexa 488 are not affected by the addition of 1wt.% Trehalose. A thin film was prepared by spin casting 40 μL of the Cyt*c*-A488 solution onto a microscope cover slip and was dried in air. Denatured Cyt*c*-A488 in a 1% trehalose film was prepared by spin casting with Cyt*c*-A488 solutions in a 100 mM phosphate buffer (pH 7.0) containing GdHCl at various concentrations.

On the other hand, we have measured the fluorescence lifetimes of single-Cyt*c*-A488 and Alexa 488 in the absence of a denaturant. The fluorescence lifetimes of the folded Cyt*c*-A488 and Alexa 488 embedded in the trehalose film were determined to be 0.37 ns and 3.72 ns, respectively (See Fig. S10b). These lifetimes are similar to those of Cyt*c*-A488 and Alexa 488 measured in the bulk experiment within the experimental error.

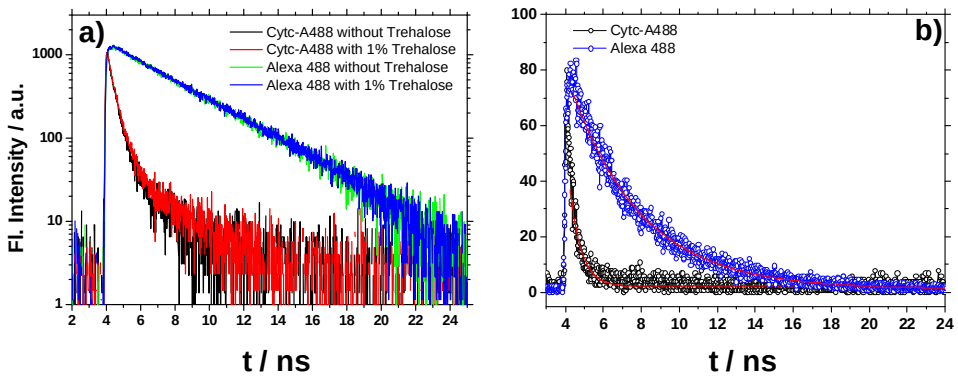

Fig. S10. a) Trehalose effect on the fluorescence lifetimes of Cyt*c*-A488 and Alexa 488 with and without GdHCl in 100 mM phosphate buffer solutions. b) Fluorescence decay profiles of Cyt*c*-A488 (black) and Alexa 488 (blue) embedded in the trehalose film (λ_{Ex} = 485 nm). The theoretical fits obtained from the fitting analysis are shown in red.

Fluorescence intensity trajectories of Cytc-A488 and Alexa 488

Fig. S11 exhibits typical fluorescence intensity trajectories (FITs) of single-molecule Cyt*c*-A488 with various GdHCl solutions in 100 mM phosphate buffer (pH 7.0). As shown in Fig. S11, the FITs of Cyt*c*-A488 with various GdHCl solutions exhibit one-step photo-bleaching and on-off blinking behaviors, which are characteristic features of a single-molecule. Especially, FITs of Cyt*c*-A488 in the trehalose film containing the small amount of GdHCl (≤1.0M) shows the strong fluctuation compared with that of single-molecule Alexa 488 on a glass coverslip, indicating that PET in the same protein take place substantially between Alexa 488 and amino acids such as Trp, and the PET in the folded state of a protein is much more efficient than in the denatured state.

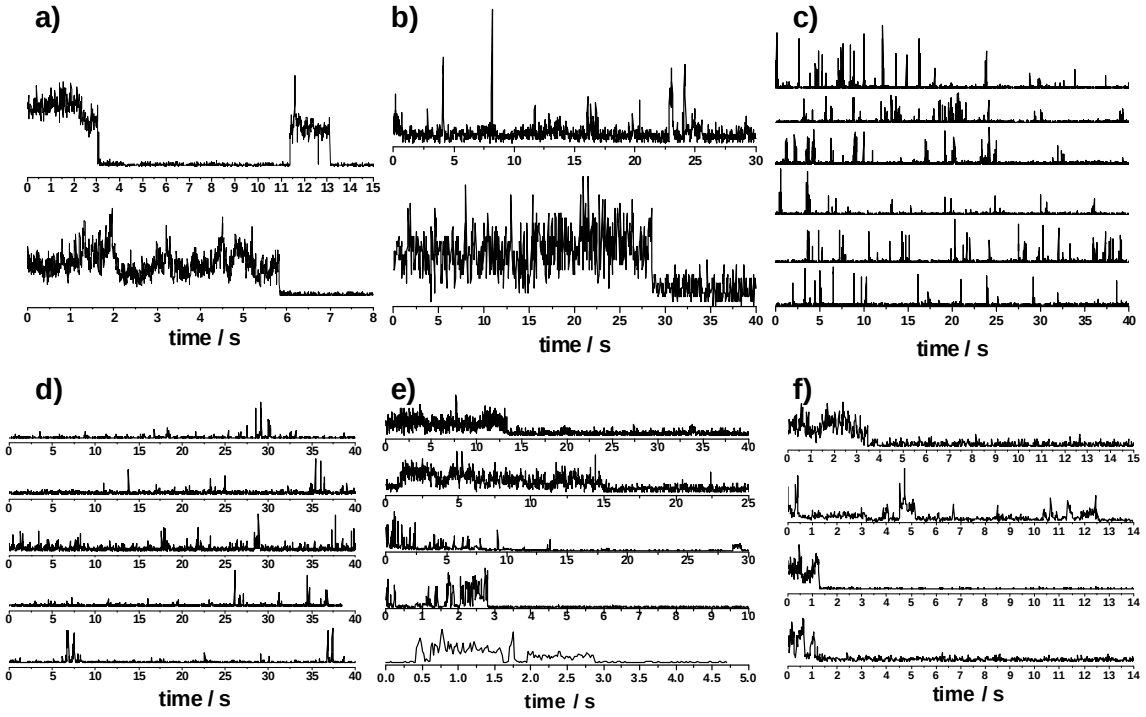

Fig. S11. Typical fluorescence trajectories of single-molecule Alexa 488 (a) in buffer solutions without a denaturant and Cytc-A488 (b-f) with various concentrations of GdHCl. b-f) [GdHCl]= 0.0, 0.5, 1.0, 2.0 and 4.0 M.

Fluorescence Correlation Spectroscopy (FCS)

In order to elucidate the contribution of the singlet-triplet relaxation of Alexa 488 in the FCS curve of Cyt*c*-A488, we observed the FCS curve for Alexa 488 at various concentrations of GdHCl at room temperature. However, we could not observe any dynamics due to the singlet-triplet relaxation as depicted in Fig. S12a. Furthermore, in FCS experiment free Alexa 488 did not show fast dynamics (< 0.01 ms) in the presence of BSA and Tween-20 (See Fig. S12b). Thus, we did not consider the contribution ofthe singlet-triplet relaxation of Alexa 488. Mukhopadhyay et al. also reported that in the FCS experiment, no fast component (< 0.01 ms) was observed for free Alexa 488 in buffer.[8]

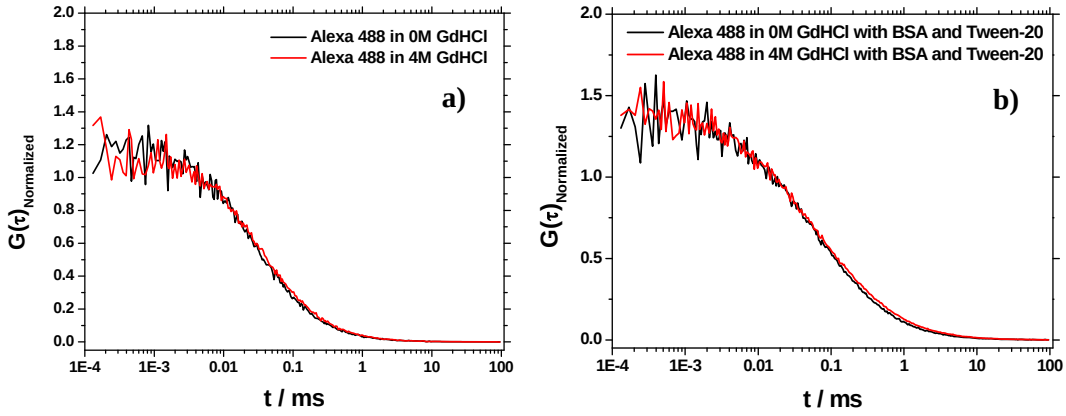

Fig. S12. a) FCS data recorded from Alexa 488 at various concentrations of GdHCl at room temperature. b) FCS data recorded from Alexa 488 with BSA and Tween-20 at various concentrations of GdHCl at room temperature.

References

(1) Mei, E.; Tang, J.; Vanderkooi, J. M.; Hochstrasser, R. M. *J. Am. Chem. Soc.* **2003**, *125*, 2730-5.

(2) Chen, H.; Ahsan, S. S.; Santiago-Berrios, M. B.; Abruna, H. D.; Webb, W. W. *J. Am. Chem. Soc.* **2010**, *132*, 7344-45.

(3) Neuweiler, H.; Johnson, C. M.; Fersht, A. R. *Proc. Natl. Acad. Sci. U S A.* **2009**, *106*, 18569-74.

(4) Widengren, J.; Mets, U.; Rigler, R. *J. Phys. Chem. B* **1995**, *99*, 13368-13379.

(5) Bonnet, G.; Krichevsky, O.; Libchaber, A. *Proc. Natl. Acad. Sci. U S A* **1998**, *95*, 8602-6.

(6) Levene, M. J.; Korlach, J.; Turner, S. W.; Foquet, M.; Craighead, H. G.; Webb, W. W. *Science* **2003**, *299*, 682-6.

(7) Ries, J.; Yu, S. R.; Burkhardt, M.; Brand, M.; Schwille, P. *Nat. Methods* **2009**, *6*, 643-5.

(8) Mukhopadhyay, J.; Kapanidis, A. N.; Mekler, V.; Kortkhonjia, E.; Leroy, O.; Ebright, Y. W.; Weiss, S.; Ebright, R. H. *Biophys. J.* **2002**, *82*, 115a-116a.